Physica D 238 (2009) 1897–1908

Contents lists available at ScienceDirect

Physica D

journal homepage: www.elsevier.com/locate/physd

A single particle impact model for motion in avalanches

J.J.P. Veerman [a,b], D. Daescu [a], M.J. Romero-Vallés [b], P.J. Torres [b,*]

[a] Department of Mathematics and Statistics, Portland State University, Portland, OR 97207, United States
[b] Departamento de Matemática Aplicada, Universidad de Granada, Granada, 18071, Spain

ARTICLE INFO

Article history:
Received 24 April 2008
Received in revised form
9 June 2009
Accepted 15 June 2009
Available online 24 June 2009
Communicated by G. Stepan

Keywords:
Impact system
Granular flow
Periodic orbit

ABSTRACT

We describe the global behavior of the dynamics of a particle bouncing down an inclined staircase. For small inclinations all orbits eventually stop (independent of the initial condition). For large enough inclinations all orbits end up accelerating indefinitely (also independent of the initial conditions). There is an interval of inclinations of positive length between these two. In that interval the behavior of an orbit depends on its initial condition. In addition to stopping and accelerating orbits, there are also orbits with speeds bounded away from both zero and infinity. A second hallmark of the dynamics is that the orbits going at a finite (but non-zero) average speed tend to have close to constant speed. In the setting of this model these phenomena are robust in the sense that they are independent of the 'ruggedness' of the staircase and of the coefficients of restitution that govern the energy loss at each bounce.

The behavior just described matches up well with physical observations of single particles falling down a rough slope as well as measurements in laboratory controlled avalanches. This (and the robustness of the results) suggests that many-particle systems (avalanches) behave in similar ways as our low-dimensional model.

1. Introduction

One major difficulty of impact dynamics, is that a part of it is not continuous and for that reason very little of its global dynamics is known. Impact systems and related systems (such as the buck converter, granular media) have a very wide applicability. For example it has been estimated [1] that half of the products of the chemical industry are in granular form. But relatively little is known about the global aspects of its dynamics.

In this work we investigate an impact system with remarkable properties. It is a highly idealized model of the dynamics of a grain going down a pile of granular material, its motion driven by gravity. A major motivation for this model came from the study of avalanches and its relation with granular dynamics. The idealization consists of a point particle falling down a inclined staircase. Related low-dimensional models are discussed in [2–4]. Those models are either simplifications of the current one and can be fully analyzed, or are limiting cases (in [3]). While these other models exhibit interesting behavior, and in fact compare well with some physical experiments as in the case of [5], they do not have the behavior that we describe now and that is characteristic for avalanches of granular material.

The model studied here is simple enough so that it is accessible by analytical methods. But it also sufficiently complicated that its dynamics is non-trivial and interesting; in fact, substantial questions remain to be answered. Nonetheless, we argue that this superficially very simple low-dimensional dynamical system *mimics* the behavior of physical avalanches in at least two important aspects.

In experimental granular systems (such as dry sand) it turns out that when one pours it on a pile, there is a well-defined interval of angles with the following properties (see [6]). Below the smallest angle of the interval, called the angle of repose, avalanches tend not to occur. The largest angle is called the angle of maximal stability; above it an avalanche will always diminish the local slope. The model we discuss exhibits a dynamics that is very reminiscent of this. The main parameter is the angle of inclination ϕ of the staircase (see Fig. 2.1). Indeed we argue that

1. for values of ϕ below a certain threshold ϕ_∞, a falling particle will eventually always stop,
2. while for angles bigger than a threshold $\phi_s > \phi_\infty$ the particle always accelerates (as in an avalanche), such that its velocity tends to infinity.
3. In the interval in between these, both are possible, as are orbits with velocities bounded away from both zero and infinity. In this case the ultimate behavior depends on the initial condition.

Thus we see that this peculiar behavior of many-particle avalanches, is also a characteristic of our single particle model. In the

* Corresponding author.
E-mail address: ptorres@ugr.es (P.J. Torres).

0167-2789/$ – see front matter © 2009 Elsevier B.V. All rights reserved.
doi:10.1016/j.physd.2009.06.017

setting of this model these phenomena are robust in the sense that they are independent of the 'ruggedness' of the staircase and of the coefficients of restitution that govern the energy loss at each bounce.

The second remarkable aspect about this system with physical implications is that it appears to have a strong preference for (bounded) orbits that are closely related to circular rotations. The system has a certain tendency to select orbits whose speed is close to constant. This implies that particles going at the same average speed in an avalanche tend to have nearly constant velocity. In this way the number of collisions between particles in an avalanche are minimized as well as their relative momentum when they *do* collide. Both of these factors mean that energy loss due collision between particles is minimal.

Commonly this kind of phenomenology is studied in the context of — and thus associated with — large numbers of interacting particles (see [7,8,6,9–12]). In these studies one of the main questions is, what is the distribution of the sizes of the avalanches? Important exceptions are [13,12,14,15] and related models such as [16] for sand transportation by wind. Due to technical difficulties even in the detailed modeling for the single particle problem (see for instance [17,18]), these results are numerical or experimental in nature.

Non-smooth dynamics is a broad research area attracting the interest of an increasing number of mathematicians, physicians and mechanical engineers. The reason for this growing interest is, on one hand, the ubiquity of this type of process in the applications and, on the other hand, that a general theoretical frame is far from being available if compared with the theory of smooth dynamical systems. Most, if not all, powerful theorems require the system to have some regularity (continuity if not differentiability). This provides us with another powerful motivation to study such systems in depth about which very little is known in general.

Mathematically, a non-smooth process is described by a differential system with discontinuities. Following [19], discontinuous systems can be classified into three types according to their degree of discontinuity:

1. Systems with a discontinuous Jacobian: the vector field is continuous but not differentiable. An example is the asymmetric oscillator (see for instance [20,21] and the references therein), which is a relevant model to understand oscillations of suspension bridges [22].
2. Differential systems with a discontinuous right-hand side. The vector field is discontinuous and the solutions must be understood in the sense of Filippov [23]. Some examples are oscillators with dry friction [24–26] or switching systems like the DCDC-buck converter [27].
3. Systems with discontinuities in the state, like impacting systems with velocity reversals. The model studied in this paper falls into this category. Theoretically, the study of this type of systems presents the difficulty that there is not a well-established theory about existence and prolongation of solutions. Models with impacts appear naturally in a wide range of applications like particle accelerators [28], dynamics of structures under the action of earthquakes [18] or percussion machines and print hammers [29]. The dynamics of billiards is a broad and interesting area [30]. More specifically, the model under study in this paper can be seen as a gravitational billiard [31,32]. A general exposition of the subject as well as a large number of references to other applications can be found in the review [33] and the books [34,35].

We thus have a class of low-dimensional dynamical impact systems exhibiting a very distinctive behavior, that is commonly associated with systems of many interacting particles. In spite of the inherent difficulty of these systems, we obtain a reasonably complete picture of its dynamics, a large part of which we can prove.

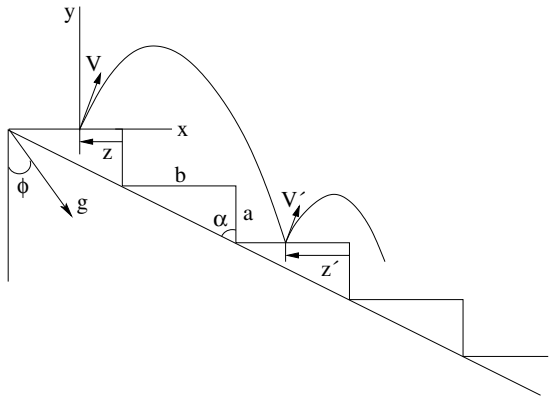

Fig. 2.1. The model (Figure from [36]).

In what follows we give a detailed description of the model, the main theorems as well as the main conjecture, in Section 2. Here we also present the numerical evidence for the main Conjecture. In Section 3 we prove that all periodic orbits are attractors (a result announced in [36,4]). Sections 4 and 5 contain the main results. In the first part we supply the partial proof of the Conjecture and in the other two we make a detailed study of periodic orbits.

2. The model and the main results

In this section we define the model, give the main results, and specify what we can prove. Full details and proofs appear in subsequent sections. The numerical evidence of the Main Conjecture (Conjecture 2.2) is also given in this section.

The model consists of a particle bouncing down a staircase as depicted in Fig. 2.1. The steps of the staircase are rectangular (with sides of length a and b) and the staircase itself is forward inclined over an angle ϕ. We always assume that the particle falls at least one step during its orbit (the other orbits being trivial). The particle has initial conditions $\mathbf{V} = (u, v)$, its velocity, and position z (see Fig. 2.1). These three coordinates define the dynamical space. The coordinates of the parameter space consist of the two restitution coefficients e_t (tangential) and e_n (normal). In general momentum is not conserved during a collision. This is true for the momentum perpendicular to the collision plane (hence $e_n \in (0, 1)$) as well as the momentum tangential to it (hence $e_t \in (0, 1)$ (see for example [37]). We have used these same conventions for example in [36]. The parameter $\kappa \equiv \frac{a}{b} \tan\phi$ which we call 'inclination' after the angle ϕ at which the staircase is tilted (see the figure).

Upon launching the particle goes in a ballistic orbit with initial conditions $(u, v, x = 0, y = 0)$ until it collides with the staircase at some $y = -na$. At this point the coordinates of the particle are determined by:

$$\begin{aligned} u_c &= u + gst \\ v_c &= v - gct \\ x_c &= ut + \frac{1}{2}gst^2 \\ y_c &= vt - \frac{1}{2}gct^2 = -na. \end{aligned} \tag{2.1}$$

We have defined the parameters $s \equiv \sin\phi$ and $c \equiv \cos\phi$. The number n is called the jump number. These equations can be solved for the time of flight t. The initial conditions at the start of the next jump are then determined by the law of restitution at the point of collision:

$$\begin{aligned} u' &= e_t u \\ v' &= -e_n v. \end{aligned}$$

Here (u, v) is the velocity of the particle just before landing and (u', v') just after. The coefficient of restitution greatly influences the dynamics of a particle (see for example [38]). Since in applications, these may not be known or may vary, we keep these as parameters.

It is convenient to write out the final equations in a different set of coordinates:

$$X = \frac{x}{b}, \qquad Y = \frac{y}{a}, \qquad Z = \frac{z}{b},$$
$$U = \frac{c}{s}\frac{u}{\sqrt{2gca}}, \qquad V = \frac{v}{\sqrt{2gca}}, \qquad T = \sqrt{\frac{gc}{2a}}. \tag{2.2}$$

This change of coordinates is singular at $\phi = 0$. This case, $\phi = 0$, is an interesting special case, with its own particularities, and is studied independently in [3]. We subsequently drop the cap notation and introduce the parameter:

$$\kappa \equiv \frac{sa}{cb}.$$

It is easy to integrate the above equations (by first solving for the time of flight) to get the dynamical system F which expresses the velocity and position (u', v', z') at take-off in terms of those at the previous take-off, (u, v, z). Thus for each value of the parameters the above dynamical system F is in fact a map $F_{e_t,e_n,\kappa} : \mathbb{R}^+ \times \mathbb{R}^+ \times [0, 1-\kappa) \to \mathbb{R}^+ \times \mathbb{R}^+ \times [0, 1-\kappa)$ given by:

$$\begin{aligned} u' &= e_t[u + v + \sqrt{v^2 + n}] \\ v' &= e_n\sqrt{v^2 + n} \\ z' &= n(1-\kappa) + z - 2\kappa(u+v)(v + \sqrt{v^2+n}) \end{aligned} \tag{2.3}$$

where n is determined by the requirement that

$$n \text{ smallest non negative integer such that } z' \geq 0. \tag{2.4}$$

It is clear from the above equations that such an n exists. Note that the velocity components are assumed to be non-negative. We assume that if both components are zero, then the particle rests and does not jump (this is consistent with the above equations). Of course z' will be largest in a near vertical (parallel with gravity) fall. This happens for example when $z = 0$ and u and v tend to zero. One verifies that $z' < 1 - \kappa$.

We will make use of the following.

Observation: We have

$$\frac{(\kappa u + v)^2}{1-\kappa} \geq 4\kappa v(u+v) \quad \text{since}$$
$$(\kappa u + v)^2 - (1-\kappa)4\kappa v(u+v) = (\kappa(u+2v) - v)^2 \geq 0.$$

Inspection of Eq. (2.3) easily leads to the conclusion that

$$n = 0 \quad \text{if and only if } z \geq 4\kappa v(u+v), \tag{2.5}$$

and if that condition does not hold, the jump number is determined by

$$n = \text{ceil}\,\{Q(u, v, z)\} \quad \text{where}$$
$$Q(u, v, z) \equiv \frac{2\kappa(u+v)}{(1-\kappa)^2}\left[\kappa u + v + \sqrt{(\kappa u + v)^2 - (1-\kappa)z}\right] - \frac{z}{1-\kappa}. \tag{2.6}$$

(For future reference we note that the above observation implies that whenever $n > 0$, the term under the root is non-negative.) Due to the discontinuities $DF(\xi_0)$ is not defined for values ξ_0 such that $Q(\xi_0) \in \mathbb{N}$. Extend the definition by allowing DF to be the unique linear operator defined on all of X as satisfying

$$F(\xi(t)) - F(\xi_0) = DF(\xi_0)\cdot(\xi(t) - \xi_0) + \mathcal{O}(|\xi(t) - (\xi_0)|^2)$$

only along (differentiable) paths $\xi(t)$ with $\xi(0) = \xi_0$ and such that $Q(\xi(t)) \geq Q(\xi_0)$ (paths of constant n). We will use this extension throughout the paper wherever necessary.

Throughout this paper we will denote the dynamical space $\mathbb{R}^+ \times \mathbb{R}^+ \times [0, 1-\kappa)$ by X and the parameter space $(0, 1)^3$ by P. One of our main interests is to understand the so-called criterion map. This map, $\sigma : X \times P \to \{\text{I, II, III}\}$, assigns to each initial condition in $\xi \in X$ and each parameter value in $p \in P$ an element in {I, II, III} according to the following criterion:

The orbit with initial condition (ξ, p) eventually stops
  then $\sigma(\xi, p) = \text{I}$.
The velocity of the orbit with initial condition (ξ, p) tends to
  infinity then $\sigma(\xi, p) = \text{III}$.
else then $\sigma(\xi, p) = \text{II}$.

The characterization of the dynamics of this system is summarized in the following Theorem and Conjecture. The first has been proved in [36] and the second has been stated in [36,4], and numerical evidence has been collected here in Figs. 2.2 and 2.3. It is one of the main open questions for this class of models and will be partially proved in Section 5.

Theorem 2.1. *Let $\xi = (u, v, z) \in (\mathbb{R}^+)^2 \times [0, 1-\kappa) = X$ and $p = (e_t, e_n, \kappa) \in (0, 1)^3 = P$. There are smooth surfaces*

$$\kappa = \kappa_\infty(e_t, e_n) \equiv \frac{(1-e_t)(1-e_n)}{(1+e_t)(1+e_n)} \quad \textit{and}$$
$$\kappa = \kappa_s(e_t, e_n) \equiv \frac{1 - e_t e_n - e_n^2 + e_t e_n^3}{1 + 3e_t e_n + 3e_n^2 + e_t e_n^3} \tag{2.7}$$

in P with the following properties:

$$0 \leq \kappa_\infty(e_t, e_n) \leq \kappa_s(e_t, e_n) \leq 1$$

where equality is only possible in the boundary of $[0, 1]^2$. Furthermore,

(i) $\kappa < \kappa_\infty \Rightarrow \sigma(\xi, p) \in \{\text{I, II}\}$
(ii) $\kappa_\infty \leq \kappa \leq \kappa_s \Rightarrow \sigma(\xi, p) \in \{\text{I, II, III}\}$ & *orbits of all three types occur*
(iii) $\kappa > \kappa_s \Rightarrow \sigma(\xi, p) \in \{\text{II, III}\}$.

Conjecture 2.2. $\sigma(\xi, p) = \text{II}$ *only if* $\kappa_\infty \leq \kappa \leq \kappa_s$.

We present our numerical evidence for the Conjecture, see Figs. 2.2 and 2.3. In the first e_t is fixed at 0.2. Then a 1000×1000 grid is laid out in the (e_n, κ) plane (with $e_t = 0.2$). For each of these values of (e_t, e_n, κ), 10.000 initial conditions (u_0, v_0, z_0) are tested. These have $z_0 = 0$, but the angle of the initial condition (u_0, v_0) is randomly distributed between 0 and $\pi/2$ (uniform distribution) while the norm of the velocity, $|(u_0, v_0)|$, is distributed according to a cumulative probability distribution proportional to $\arctan(\sqrt{u_0^2 + v_0^2})$. Each of these initial conditions is iterated to decide whether the orbit eventually stops, accelerates indefinitely or maintains a finite velocity. The numerical criterion for convergence to infinity is that each iterate the speed grows with the factor $\lambda_+ > 1$ is the greater of the eigenvalues referred to in Eq. (4.3). The criterion for a stopping orbit is that the 'stopping distance' (given in Lemma 2 of Section 4 in [36]) is smaller than or equal to the distance remaining to the edge of the current ramp. *If, after a certain number of iterates, the orbit fails to satisfy either of the these criteria, it is assigned the label "bounded".* A pixel is colored dark blue, if *all* initial conditions corresponding to it tend to stop, and light blue if *all* tend to accelerate forever. Orange is reserved for those pixels where all initial conditions lead either to a halt *or* indefinite acceleration. Any other color indicates, that at least one of the 10,000 initial conditions generates an orbit that fails both

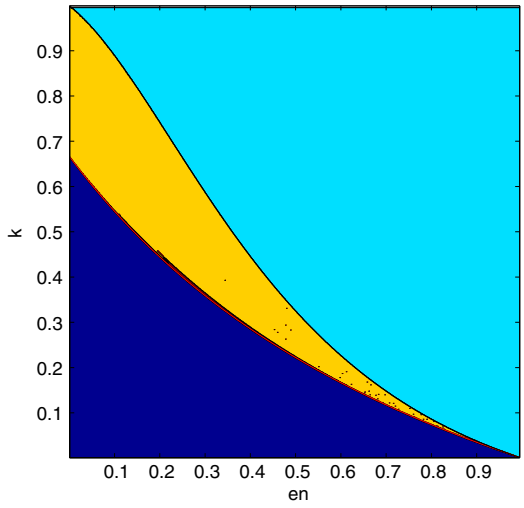

Fig. 2.2. e_t is held fixed at 0.2. Orbits tend to go always to zero in one region (dark-blue), to infinity in another (light-blue), whereas both are possible in the middle region (orange). Each pixel represents 10,000 orbits. If a single bounded, but non-zero orbit was found in 10,000 trials, the pixel receives a different color. Only some dust in the lower of the middle region is visible. (For interpretation of the references to colour in this figure legend, the reader is referred to the web version of this article.)

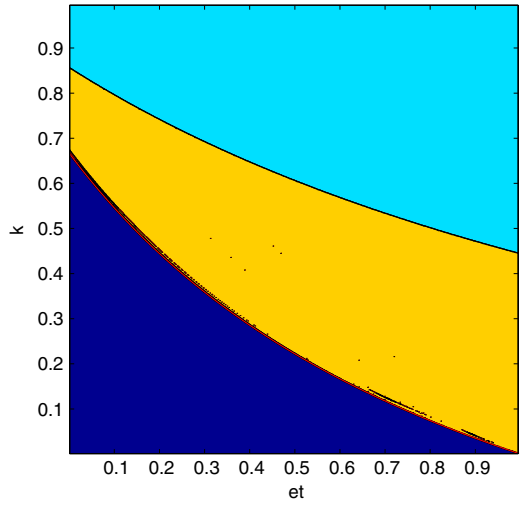

Fig. 2.3. The figure is generated as Fig. 2.2, with e_t and e_n exchanged, so that here e_n is held fixed at 0.2.

these criteria. In the second figure the conventions are the same but now $e_n$is held fixed at 0.2 instead of e_t.

The conclusion from these numerical experiments is pretty clear. Below a surface $\kappa = \kappa_s(e_t, e_n)$ all orbits eventually come to a halt and above it none do. In other words: orbits with inclination less than $\kappa = \kappa_s(e_t, e_n)$ always stop. Above the surface $\kappa = \kappa_\infty(e_t, e_n)$, which is strictly bigger than $\kappa = \kappa_s(e_t, e_n)$, all orbits have speeds that tend to infinity speed and below it none do. Orbits with bounded but non-zero speed are exclusively possible between these two inclinations. They appear to be rare; there is only some dust visible in the middle and lower parts of the orange regions. The boundaries of these regions coincide with the boundaries predicted by the theory (see below) to within numerical precision.

3. Periodic orbits attract

In this section, we show that every periodic orbit of the system has a small interval of translates of it associated to it, and that this one-parameter set of periodic orbit thus formed attracts an open set of initial conditions. (This notion of 'attractiveness' we use is detailed in the course of stating the Proposition below.) This result was earlier stated (but not proved) in [36].

Fix the parameters. Suppose the system has a k-periodic orbit which we will denote by $\mathcal{O}$. By this we mean an orbit $\{(u_i, v_i, z_i)\}_{i=0}^{k-1}$ of Eq. (2.3) satisfying Eq. (2.4) whose least period equals k. From the geometry of the problem it follows that $\{z_i\}_{i=0}^{k-1}$ must lie in the half open interval $[0, 1-\kappa)$. We choose z_0 to be the smallest of the $\{z_i\}$. We now have the following result.

Proposition 3.1. *Suppose the system has a k-periodic orbit $\mathcal{O} \equiv \{(u_i, v_i, z_i)\}_{i=0}^{k-1}$. Denote by D_r the open disk in the plane of radius r centered at (u_0, v_0). There exists a real number $z_\mathcal{O} > 0$ which is maximal with respect to the property that for all p, q with $0 < p < q < z_\mathcal{O}$, there is an $r > 0$ such that every initial condition in the open set $U \equiv D_r \times (p, q) \subset X$ converges exponentially fast under F to a z-translate of the original periodic orbit.*

Proof. Fix the initial condition $\xi_0 = (u_0, v_0, z_0)$ of the k-periodic orbit so that $z_0 = \min_{i=0}^{k-1} z_i$. Assume that Eq. (2.5) is not satisfied at ξ_0. Eq. (2.3) implies that if we start with the initial condition (u_0, v_0, z_0') and the n_i do not change, then the new orbits is a z-translate of the old one (we call this 'local translational invariance').

We first construct $z_\mathcal{O}$. As a function of z, n is continuous from the right and piecewise constant. Thus there is a $\delta > 0$ such that for $z_0' \in [z_0, z_0 + \delta)$, n_0 is constant. By taking δ smaller if necessary the same applies to the subsequent n_i for $i \in \{0, \ldots, k-1\}$. On the other hand if we set $0 \le z_0' < z_0$, then again according to Eq. (2.6) upon choosing (u_0, v_0, z_0') as new initial condition, n_0 can at best increase (because Q is a decreasing function of z). However, that would contradict Eq. (2.4). Thus for every z_0 chosen as indicated there is an interval $I = [0, z_0 + \delta)$ so that for all initial conditions (u_0, v_0, z) with $z \in I$ the value of n equals n_0. The same applies to n_i for $i \in \{0, \ldots, k-1\}$. Thus, by local translational invariance, the orbit of (u_0, v_0, z) is a translate of $\mathcal{O}$. We set $z_\mathcal{O}$ to be the supremum of the values of z_0 for which the above holds. (One can check that this reasoning also holds if Eq. (2.5) is satisfied.)

Choose p and q as in the Proposition. Choose further p' and q' satisfying $0 < p' < p < q < q' < z_\mathcal{O}$. Consider again Eq. (2.6). The open condition: $Q(u_i, v_i, z_i) \notin \mathbb{N}$ for $i \in \{0, \ldots, k-1\}$ is satisfied for all (u_0, v_0, z) with $z \in (p', q')$ and thus there is an $\epsilon > 0$ so that it is satisfied in $D_\epsilon \times (p', q')$. On $D_\epsilon \times (p', q')$ the functions $\{F^i\}_{i=1}^k$ are (formally) differentiable, since the n_i are constant. By choosing ϵ smaller, if necessary, we can set things up so that $D_\epsilon \times (p', q')$ contains an ϵ-neighborhood of $\{\cup_{z\in(p,q)}(u_0, v_0, z)\}$.

According to the previous the derivative of the map F given in Eq. (2.3) always exists and is uniformly bounded on $\cup_{i=0}^{k-1} F^i(D_\epsilon \times (p', q'))$. The derivative satisfies (see [36]):

$$DF^i = \begin{pmatrix} e_t^i & * & 0 \\ 0 & e_n^{2i} & 0 \\ ** & * & 1 \end{pmatrix}.$$

Here $*$ stands for an arbitrary entry. The eigenvalues of this matrix are its diagonal entries. The projection of F onto the velocity plane does not depend on z and has a hyperbolic attracting periodic orbit given by $\{(u_i, v_i)\}$. As a consequence for $\theta \in (e_t, 1) \cap (e_n^2, 1)$, there is a K such that:

$$|(u_i', v_i') - (u_i, v_i)| < K\theta^i |(u_0', v_0') - (u_0, v_0)|. \tag{3.1}$$

Denote

$$L \equiv \sup_{x \in \text{closure}\left\{\cup_{i=0}^{k-1} F^i(D_\epsilon \times (p,q))\right\}} \|DF(x)\|.$$

Choose (u_0', v_0', z_0) in $D_r \times (p, q)$, where r is smaller than ϵ and chosen such that

$$\frac{2LKr}{1-\theta} < \epsilon. \tag{3.2}$$

We prove that every orbit with initial condition in $D_r \times (p, q)$ is attracted to a k-periodic orbit.

Let $\{\xi_i\} = \{(u_i, v_i, z_i)\}$ be the original k-periodic orbit with $z_0 \in (p, q)$. Furthermore, $\{\xi_i'\} = \{(u_i', v_i', z_i')\}$ is an orbit with initial condition in $D_r \times \{z_0\}$ (note that $z_0' = z_0$). Taylor's Theorem applied to the third component of Eq. (2.3) says that for all $j > 0$:

$$\begin{aligned} z_{j+1}' = z_j + n_j(1-\kappa) - 2\kappa(u_j + v_j)\left(v_j + \sqrt{v_j^2 + n_j}\right) \\ + R_1(u_j', v_j', z_j')(u_j' - u_j) + R_2(u_j', v_j', z_j')(v_j' - v_j) \\ + R_3(u_j', v_j', z_j')(z_j' - z_j). \end{aligned}$$

Here, of course, the remainder terms are estimated by $|R_i| \le L$ for $i = 1$ and $i = 2$. However, for $i = 3$ we have $R_3 = 1$. Thus with the help of Eq. (2.3) we get:

$$\begin{aligned} z_{j+1}' - z_{j+1} = z_j' - z_j + R_1(u_j', v_j', z_j')(u_j' - u_j) \\ + R_2(u_j', v_j', z_j')(v_j' - v_j). \end{aligned}$$

And thus

$$\begin{aligned} |z_{j+1}' - z_{j+1}| &\le |z_j' - z_j| + 2L|(u_j', v_j') - (u_j, v_j)| \\ &\le 2L\sum_{i=0}^{j} K\theta^i r < \frac{2LKr}{1-\theta} < \epsilon. \end{aligned}$$

(We used Eq. (3.1) to obtain the second inequality and Eq. (3.2) for the last one.) This implies that $F^{ik}(\xi_0')$ (where k is the period) never leaves the ϵ neighborhood of $\{\cup_{z\in(p,q)}(u_0, v_0, z)\}$, and the same of course is true for its images $F^{ik+j}(\xi_0')$ under F. ■

Remark. We will from now simply say that the set of periodic orbits thus described forms an 'attractor', though this is not, strictly speaking, the usual convention (see [39,40] for details about the notion of attractor).

4. The attractors at zero and infinity

Recall that if $\kappa > \kappa_\infty$, then every orbit with a large enough initial speed will have the property that the limit of its speed tends to infinity, and if $\kappa < \kappa_s$, there are always stopping orbits (in fact, that is the definition of κ_s, see [36]). Here we refine this statement. In the first case, we exhibit a specific neighborhood of infinity all of whose orbits are attracted to infinity. In the second case, we exhibit an explicit upper bound on the limsup of the velocity of any orbit. Together these statements form a partial confirmation of Conjecture 2.2.

From [36] we have the following result.

Proposition 4.1. *The dynamical system F can be rewritten as:*

$$\begin{aligned} u' &= \frac{e_t}{1-\kappa}\big[(1+\kappa)u + 2v\big] + e_t\gamma(u, v), \\ v' &= \frac{e_n}{1-\kappa}\big[2\kappa u + (1+\kappa)v\big] + e_n\gamma(u, v), \end{aligned} \tag{4.1}$$

$$\text{where } \gamma(u, v) \equiv \sqrt{v^2 + n} - \frac{2\kappa u + (1+\kappa)v}{1-\kappa}, \tag{4.2}$$

and γ tends to zero as the velocities get large (see Proposition 4.2). The characteristic polynomial of the linearized system associated with Eq. (4.1)

$$p(\lambda) = \lambda^2 - (e_t + e_n)\frac{(1+\kappa)}{(1-\kappa)}\lambda + e_t e_n, \tag{4.3}$$

has a real root greater than 1 if and only if $\kappa > \kappa_\infty$ (see Eq. (2.7)).

The next proposition is a slight extension of results mentioned in [36] (for which reason we include a proof).

Proposition 4.2. (i) *Let $(\kappa u+v)^2 \ge (1-\kappa)z$. Then $\gamma(u, v)$ satisfies:*

$$-1 \le -\frac{1-\kappa}{2(\kappa u + v)} \le \gamma(u, v).$$

(ii) *$\gamma(u, v)$ always satisfies:*

$$\gamma \le \min\left\{1, \frac{1-\kappa}{2(\kappa u + v)}\right\}.$$

(iii) *Let $(\kappa u + v)^2 < (1-\kappa)z$. Then $n = 0$ and*

$$\gamma = -\frac{2\kappa(u+v)}{1-\kappa}.$$

Proof. To prove the second inequality in part (i), substitute the first inequality of Equation (14) of [36] into Eq. (4.2) to get that:

$$\begin{aligned} \gamma &\ge \frac{\kappa u + v}{1-\kappa}\left(\sqrt{1 - \frac{(1-\kappa)z}{(\kappa u + v)^2}} - 1\right) \\ &\ge -\frac{\kappa u + v}{1-\kappa}\left(\frac{(1-\kappa)z}{(\kappa u + v)^2}\right). \end{aligned}$$

Then recall that $z < 1 - \kappa$. The first inequality is obtained by also using the condition given in this statement.

To prove (ii): First set

$$n = \left(\left(\sqrt{v^2 + n}\right)^2 - v^2\right)$$

and substitute this into the first n of the third line of Eq. (2.3). Subsequently from Eq. (4.2) we get

$$\sqrt{v^2 + n} = \gamma(x) + \frac{2\kappa}{1-\kappa}u + \frac{1+\kappa}{1-\kappa}v,$$

and substitute this again in the equation. We then obtain (after considerable algebra)

$$z' - z = \gamma(x)\Big(\gamma(x)(1-\kappa) + 2(\kappa u + v)\Big).$$

Both z and z' are in $[0, 1-\kappa)$. Setting $z' - z < 1 - \kappa$ and solving the resulting quadratic inequality, we easily show that:

$$\begin{aligned} \gamma &\le -\frac{\kappa u + v}{1-\kappa} + \sqrt{\left(\frac{\kappa u + v}{1-\kappa}\right)^2 + 1} \\ &= \left(\frac{\kappa u + v}{1-\kappa}\right)\left(\sqrt{1 + \frac{(1-\kappa)^2}{(\kappa u + v)^2}} - 1\right) \\ &\le \min\left\{1, \frac{1-\kappa}{2(\kappa u + v)}\right\}. \end{aligned}$$

Here we have made use of the following inequalities for positive x:

$$\begin{aligned} -x + \sqrt{1 + x^2} &\le 1 \\ x\left(\sqrt{1 + x^{-2}} - 1\right) &\le \frac{1}{2x}. \end{aligned}$$

In Item (iii) that assertion that $n = 0$ follows from Eq. (2.5) and the Observation just prior to it. The value for γ can then be read off from Eq. (4.2). ■

It is worth pointing out that the linearization of Eq. (4.1) is a model that has been studied before in the literature [41]. It

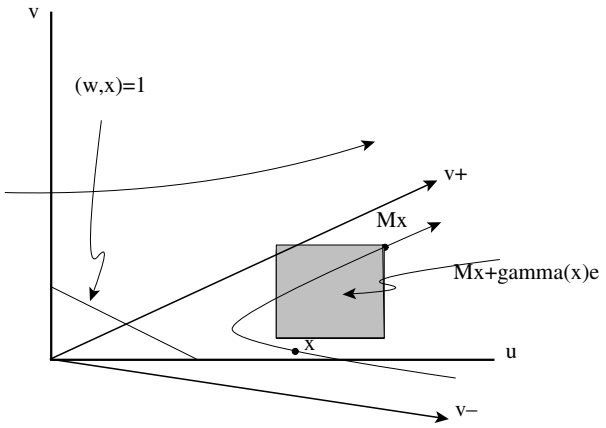

Fig. 4.1. A sketch of the dynamics in the (u, v) plane. $f(x)$ is in the gray square whose sides have lengths estimated by Proposition 4.2.

corresponds to the movement of the particle if the stepsize of the staircase tends to zero — or equivalently the speed of the particle tends to infinity. The complication in the dynamics of our current model derives entirely from the presence of the (finite) steps.

From now on M denotes the 2 by 2 matrix defined by the linearization of Eq. (4.1). Denote the cone $\{(u, v) \mid uv \geq 0\}$ by C_+ and the cone $\{(u, v) \mid uv \leq 0\}$ by C_-.

Lemma 4.3. (i) *The matrix M associated with Eq. (4.1) has associated eigenvectors $v_- \in C_-$ and $v_+ \in C_+$.* (ii) *Assume $\kappa > \kappa_\infty$. The matrix M has eigenvalues $0 < \lambda_- < 1 < \lambda_+$.* (iii) *Suppose $\kappa < \kappa_\infty$. Then M has eigenvalues $0 < \lambda_- < \lambda_+ < 1$.*

Proof. A straightforward calculation gives:

$$M = \frac{1}{1-\kappa}\begin{pmatrix} e_t(1+\kappa) & 2e_t \\ 2\kappa e_n & e_n(1+\kappa)\end{pmatrix} \quad \text{and}$$
$$M^{-1} = \frac{1}{1-\kappa}\begin{pmatrix} \dfrac{(1+\kappa)}{e_t} & \dfrac{-2}{e_n} \\ \dfrac{-2\kappa}{e_t} & \dfrac{(1+\kappa)}{e_n}\end{pmatrix}. \tag{4.4}$$

It is easy to see that M maps C_+ strictly into itself and M^{-1} maps C_- strictly into itself. Now let S denote the unit circle in $\mathbb{R}^2$ and $P : \mathbb{R}^2 \setminus \{0, 0\} \to S$ the radial projection onto the unit circle. Since $C_+ \cap S$ and $C_- \cap S$ are compact, and by the previous are mapped into themselves by PM, the latter has at least a fixed point in each of these. Of course each corresponds to an eigenvector, which we denote by v_+ and v_-, respectively. Statement (ii) and (iii) easily follow from Eq. (4.3). ■

To facilitate the analysis, we introduce some more notation. The 2-dimensional system in Eq. (4.1) will be written as

$$x' = f(x) \equiv Mx + \gamma(x)e, \tag{4.5}$$

where $x = (u, v)$ is the velocity vector, $e = (e_t, e_n)$ and M is defined as before. We will furthermore take v_- and v_+ to be unit eigenvectors of M. We can decompose each vector $x = (u, v)$ as $x = x_+v_+ + x_-v_-$ in terms of its components in the v_+ and v_- direction. In the proof of Theorem 4.4 below, the linear function x_+ of x acts as a kind of Lyapunov function. Similarly we decompose the vector $e \equiv (e_t, e_n)$ as $e_+v_+ + e_-v_-$, and the vector $w \equiv (\kappa, 1)$ as $w_+v_+ + w_-v_-$. The positive quadrant defined as $\{(u, v) \mid u \geq 0 \text{ and } v \geq 0\}$ will be denoted by C_{++}. Finally for any fixed K define the following set:

$$V_K = \{x \in C_{++} | x_+ > K\}.$$

Theorem 4.4. *We use the notation just defined and, if $\kappa \neq \kappa_\infty$, set $K \equiv \frac{e_+}{2|\lambda_+ - 1|}$.*

(i): *Fix $\kappa > \kappa_\infty$. Then all initial conditions in V_{2K} and whose jump number sequences contain no zeros, iterate exponentially fast to infinity under f.*

(ii): *Fix $\kappa > \kappa_\infty$. All initial conditions in V_{4K} iterate exponentially fast to infinity under f.*

(iii): *Fix $\kappa < \kappa_\infty$. Then for every initial condition x the ω-limit set $\omega(x)$ of x under f is contained in V_{2K}^c, the complement of V_K in C_{++}.*

Proof (*See Fig. 4.1 For a Sketch of the Dynamics*). We first prove (i). Let $x \in V_{2K}$. Note that $\lambda_+ - 1 > 0$ and assert that there exists a positive δ such that

$$x_+ = \frac{e_+}{(\lambda_+ - 1 - \delta)}.$$

Assume that $n > 0$. Eq. (2.5) and the Observation just prior to it imply that the condition in Proposition 4.2(i) holds. Using that Proposition gives:

$$\begin{aligned}(f(x))_+ &= (Mx)_+ + \gamma(x)e_+ \geq \lambda_+x_+ - e_+ \\ &= (1+\delta)x_+ + (\lambda_+ - 1 - \delta)x_+ - e_+ = (1+\delta)x_+.\end{aligned}$$

From this we conclude that $(f(x))_+ \geq (1 + \delta)x_+$. The statement follows by induction.

Now we prove the second statement. In view of the last item we only need to prove an inequality if $n = 0$. We have again that $\lambda_+ - 1 > 0$. By Eq. (2.5) and the Observation, *either* the condition of Proposition 4.2(i) holds (in which case we are done) *or* we are in the case of Proposition 4.2(iii). In the latter case there is a $\delta > 0$ such that

$$x_+ = \frac{2e_+}{(\lambda_+ - 1 - \delta)}.$$

On the other hand, we have

$$(f(x))_+ = (1+\delta)x_+ + (\lambda_+ - 1 - \delta)x_+ - \frac{2\kappa(u+v)}{1-\kappa}e_+.$$

We also have that $(w, x)^2 < (1 - \kappa)z$ implies

$$-\frac{2\kappa(u+v)}{1-\kappa} > -\frac{2(w,x)}{1-\kappa} > -2.$$

Putting these three equations together gives $f(x)_+ \geq (1 + \delta)x_+$, upon which induction yields the result.

Finally we prove the third statement. Now $\lambda_+ < 1$. If $x \in V_{2K}$ we can choose $\delta > 0$ such that

$$x_+ = \frac{e_+}{(1 - \lambda_+ - \delta)}.$$

Now

$$\begin{aligned}(f(x))_+ &\leq \lambda_+x_+ + e_+ \\ &= (1-\delta)x_+ - (1 - \lambda_+ - \delta)x_+ + e_+ = (1-\delta)x_+.\end{aligned}$$

Upon induction one sees that the orbit of x must leave V_{2K}. Furthermore, if $x \in V_{2K}^c$ we have

$$x_+ \leq \frac{e_+}{(1 - \lambda_+)},$$

and

$$(f(x))_+ \leq \lambda_+x_+ + e_+ \leq \lambda_+\frac{e_+}{(1-\lambda_+)} + e_+ = \frac{e_+}{(1-\lambda_+)},$$

which shows that the orbit cannot leave V_{2K}^c. ■

We see from the above proof that if $\kappa < \kappa_\infty$, the set V^c_{2K} defines a compact trapping region for the map given in Eq. (2.3). The stopping orbits form something like a local attractor. To prove from this information that it is the *only* attractor seems hard. In fact it is somewhat reminiscent of the so-called discrete Markus–Yamabe problem (see [42]).

5. Periodic orbits

In this section we prove some general statements about periodic orbits and set up the machinery to to make a detailed study of the existence of orbits with a *given* jump number sequence.

Denote the semi-infinite sequence of jump numbers by σ. Thus for k-periodic orbits σ is a repeating sequence of non-negative integers $\{n_0, n_1, n_2, \ldots, n_{k-1}, n_0, n_1, \ldots\}$ which we denote by $\sigma = (n_0, \ldots, n_{k-1})$. We consider σ as a symbolic sequence characterizing the orbits. Multiplication with a natural number is defined entry-wise, so that $m.\sigma \equiv \{mn_0, mn_1, mn_2, \ldots\}$. For a jump-number sequence σ one can define a rotation number

$$\rho \equiv \lim_{k\to\infty} \frac{1}{k} \sum_{i=1}^{k} \sigma_i.$$

For a periodic sequence the limit clearly exists.

For $\rho \leq 1$ there is a notion of order-preserving symbolic dynamics carefully described in [43,44]. The idea is that the collection of sequences $\{0, 1\}^{\mathbb{N}}$ can be given the topology of the circle from their interpretation as real numbers in $[0, 1]$ on the base 2 and then adding the relation $\{0 = 1\}$. A simple dynamical system is obtained by considering the right shift h_r on this set. The set $\{0, 1\}^{\mathbb{N}}_\rho$ of sequences with rotation number ρ, is forward invariant under h_r. For each ρ in $[0, 1]$ there is a unique *minimal* invariant set that preserves the ordering on the circle. Any such set for a given rotation number can be explicitly constructed (as described in [43, 44]). Sequences that preserve the order on the circle under the shift h_r are called 'order preserving' and every one of the minimal sets discussed is semi-conjugate to an invariant set on the circle induced by a rotation. Details can be found in the cited papers. Visual presentations of these sets of sequences can be found in [45]. All of this can of course be extended verbatim to $\rho \in [n, n + 1]$ by considering the shift on sequences in $\{n, n + 1\}^{\mathbb{N}}_\rho$. We give some general results concerning periodic orbits and set up the machinery to study specific periodic orbits in more detail.

We first solve for a general periodic orbit with jump-number sequence $\sigma = (n_0, n_1, \ldots, n_{k-1})$. The convention is that n, u, v, and z on the right-hand side of Eq. (2.3) all have the same subscript index. Thus: $v_{\ell+1} = e_n\sqrt{v_\ell^2 + n_\ell}$ and so forth. The v equations are independent and easy to solve. By iterating we get that

$$v_{\ell+k} = v_\ell = \sqrt{e_n^{2k} v_\ell^2 + e_n^{2k} n_\ell + e_n^{2(k-1)} n_{\ell+1} + \cdots e_n^2 n_{\ell+k-1}}.$$

From this we obtain

$$v_\ell = \sqrt{\frac{\sum_{i=0}^{k-1} e_n^{2(k-i)} n_{\ell+i}}{1 - e_n^{2k}}} \quad \text{or} \quad v_\ell = \sqrt{\frac{\sum_{i=1}^{k} e_n^{2i} n_{\ell-i}}{1 - e_n^{2k}}} \quad \text{and}$$
$$\sqrt{v_\ell^2 + n_\ell} = \sqrt{\frac{\sum_{i=0}^{k-1} e_n^{2i} n_{\ell-i}}{1 - e_n^{2k}}}. \tag{5.1}$$

Using this, we get from the u equation

$$u_\ell = \frac{\sum_{i=1}^{k} e_t^i \left\{ v_{\ell-i} + \sqrt{v_{\ell-i}^2 + n_{\ell-i}} \right\}}{(1 - e_t^k)}. \tag{5.2}$$

This fixes the velocities: they are now functions of σ, e_t, and e_n only. This leads to the following result.

Theorem 5.1 (*Uniqueness*). *Let α be a finite sequence of k jump numbers. Suppose there exists an mk-periodic orbit with jump number sequence $\{\alpha, \alpha, \ldots\}$. Then this orbit is a k-periodic with jump number sequence (α) as given by Eqs. (5.1) and (5.2).*

Proof. One verifies that in analogy with Eq. (5.1), we now obtain for the mk-periodic orbit:

$$v_\ell = \sqrt{\frac{\sum_{i=1}^{mk} e_n^{2i} n_{\ell-i}}{1 - e_n^{2k}}}.$$

However, one verifies that under the square root symbol, denominator and numerator have the factor $\sum_{i=1}^{m-1} e_n^{2i}$ in common. These cancel and upon cancelation the expression is exactly the same as the one given in Eq. (5.1). The same holds for $\sqrt{v_\ell^2 + n_\ell}$.

It thus follows that v_ℓ and $\sqrt{v_\ell^2 + n_\ell}$ are k-periodic. So we can apply the same reasoning to u_ℓ (see Eq. (5.2)). ■

For example any periodic orbit with jump number sequence $\{0, 2, 0, 2, \ldots\}$ is in fact periodic with period 2.

The next step is to obtain $\kappa_\sigma(e_t, e_n)$ from the third equation of Eq. (2.3) by setting

$$\begin{aligned} \Delta z_{\ell+1} &\equiv z_{\ell+1} - z_\ell \\ &= (1 - \kappa) n_\ell - 2\kappa(u_\ell + v_\ell)(v_\ell + \sqrt{v_\ell^2 + n_\ell}). \end{aligned} \tag{5.3}$$

This fixes the Δz_i but *not* the z_i. In fact, if the Δz_i are small enough so that all z_i can fit in the right interval, this implies that there is a family of periodic orbits. Indeed the third equation of Eq. (2.3) is invariant under translation along the z-axis. Noticing that for a k-periodic orbit $\sum_{i=1}^{k} \Delta z_i = 0$, we use the last equation to get

$$\kappa_\sigma(e_t, e_n) = \frac{\sum_{i=1}^{k} n_i}{\sum_{i=1}^{k} n_i + 2\sum_{i=1}^{k} (u_i + v_i)(v_i + \sqrt{v_i^2 + n_i})}, \tag{5.4}$$

which is a function σ, e_t, and e_n only. Thus for each finite sequence σ, there is at most one value of κ given by $\kappa = \kappa_\sigma(e_t, e_n)$ for which there is an orbit with jump number sequence σ. The catch is that we do not know that these orbits really *do* exist until we check whether Eq. (2.4) holds in each of the k points of the orbits.

However something interesting can immediately be learned from these manipulations. First off, for any periodic orbit to exist, κ must be equal to a (in principle) calculable smooth function of e_t and e_n. Thus periodic orbits of any given type can at best exist in a part of parameter space which has Lebesgue measure zero. Since of course the periodic sequences form a countable set, this immediately proves the following.

Proposition 5.2. *Given any value of (e_t, e_n) the Lebesgue measure of the of (e_t, e_n, κ) where periodic orbits that exist equal zero.*

Notice however, that every collection of periodic orbits characterized by a single k-periodic sequence σ attracts a set of positive measure of initial conditions (by Proposition 3.1).

A result that will be of importance later is the following.

Lemma 5.3 (*Homogeneity*). *Let e_t and e_n and a periodic sequence σ with period at least 2 be given. Suppose that $\{u_i\}$, $\{v_i\}$, $\{\Delta z_i\}$ are solutions for a periodic orbit with periodic jump number sequence σ, then $\{\sqrt{m}u_i\}$, $\{\sqrt{m}v_i\}$, $\{m\Delta z_i\}$ is the only possible solution for a periodic orbit with sequence $m\sigma$. We have $\kappa_\sigma = \kappa_{m\sigma}$.*

Proof. Following upon inspection of Eqs. (5.1) and (5.2) for the velocity, subsequently Eqs. (5.3) and (5.4) for z and κ. ■

This result does not imply the existence of orbits with sequence $m\sigma$. To make that more precise: fix e_t, e_n and a k-periodic ($k > 2$) sequence. Set $\kappa = \kappa_\sigma(e_t, e_n)$ and *assume* that at least an orbit with jump number sequence σ exists. For that orbit we must have:

$$z_\ell = z_0 + \sum_{i=1}^{\ell-1} z_i.$$

An orbit with sequence $m\sigma$ where $m > 1$ and z-coordinates $\{z'_\ell\}_{\ell=0}^{k-1}$ must satisfy:

$$z'_\ell = z'_0 + m\sum_{i=1}^{\ell-1} z_i.$$

Since all $\{z'_\ell\}_{\ell=0}^{k-1}$ must lie in the interval $[0, 1-\kappa)$, it is clear that for m large enough there are no orbits of type $m\sigma$. (Whether given any m there are values of (e_t, e_n) such that these orbits persist, is a different question.) This is our first indication that order-preserving orbits are favored by this system! Notice that the fixed points are exceptions: they all co-exist (see [36]) at $\kappa = \kappa_\infty(e_t, e_n)$.

Proposition 5.4. *Let $\sigma : \mathbb{N} \to \mathbb{N}$ be periodic. if there is an orbit whose jump number sequence is $m\sigma$ for some $m > 0$, then for any divisor p of m there is an orbit whose jump number sequence is $p\sigma$. (In particular p can be taken to be 1.)*

Proof. This is an corollary of the above Lemma. More insightfully, this can be proved as follows. Observe that an orbit with sequence $m\sigma$ would also be an orbit of the staircase with only every mth step left and all the others removed. The initial conditions are easily derived from the initial condition of the original orbit by rescaling the equations given in (2.2). ■

As an example, consider orbits with jump number sequence $(0, 4)$. The set of (e_t, e_n) for which such an orbit exists is a subset of the set of (e_t, e_n) for which the orbit $(0, 2)$ exists (see also next section).

Finally, we describe how to check the existence of an orbit with a given k-periodic jump number sequence $\sigma = (n_0, \ldots, n_{k-1})$. Start by calculating the $\{z_i\}_0^{k-1}$ up to a translational constant (local translation invariance). That constant is then determined by the requirement that $\min_i\{z_i\} = 0$. Existence of a periodic orbit with required jump number sequence, is equivalent to the existence of this particular orbit (by Theorem 5.1). So suppose that $z_\ell = 0$ for some $\ell \in \{0, \ldots, k-1\}$. Introducing

$$i^* \equiv \min_{q\in\mathbb{N}}\{i + qk \mid i + qk \geq \ell\},$$

we note that for all $i \in \{0, \ldots, k-1\}$ we have $z_i = \sum_{\ell+1}^{i^*} \Delta z_j$. Now define for $m \in \mathbb{N}$:

$$h_i(m) \equiv \left(\sum_{j=\ell+1}^{i^*-1} \Delta z_j\right) + m(1-\kappa_\sigma) - 2\kappa_\sigma(u_{i-1} + v_{i-1})(v_{i-1} + \sqrt{v_{i-1}^2 + m}).$$

Suppose that the jump number sequence σ is given by $(n_0, \ldots, n_{k-1})$. By construction $z_i = h_i(n_i) \geq 0$. These definitions and Eq. (2.4) now imply:

Lemma 5.5. *There exists an orbit with given k-periodic jump number sequence $\sigma = (n_0, \ldots, n_{k-1})$ if and only if*

$$\forall i \in \{0, \ldots, k-1\}, \forall m \in \{0, \ldots, n_{i-1} - 1\} : h_i(m) < 0.$$

The expressions in this Lemma depend only on σ and the values of e_t and e_n.

6. Examples of periodic orbits

In [36] we showed that for any positive integer k, there is a function $\kappa_{0^k1}(e_t, e_n)$ such that an orbit with jump number sequence (0^k1) exists if and only if κ equals $\kappa_{0^k1}(e_t, e_n)$. We also showed (see the Erratum in the Appendix) that for any integer $m > 1$, for *most* pairs (e_t, e_n) there exists a value of κ such that orbits with jump number sequence $(m, m+1)$ exist (if m equals 1 or 0 we have an existence for all pairs). Here we investigate: orbits with jump number sequence (011), which is an order-preserving sequence; orbits with jump number sequence $(0m)$ for $m > 1$ which are multiples of a order preserving sequence; and orbits with jump number sequence (0011) which is neither order-preserving nor a multiple of one. We find a strong preference for order-preserving sequences. The preference could have important physical implications, as we briefly explain in the Appendix. On the other hand Theorem 6.2 implies that there exists an order-preserving jump number sequence σ in $\{0, 1\}^{\mathbb{N}}$ and pairs (e_t, e_n) for which there is no value of κ for which such an orbit exists.

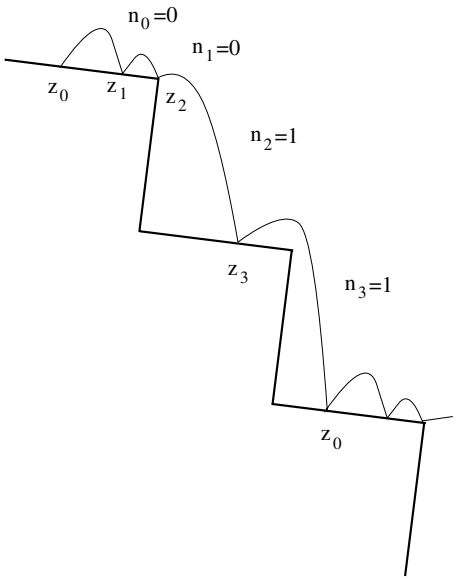

Fig. 6.1. A hypothetical (0011) periodic orbit on an inclined staircase. Note that we assume that $z_2 = 0$. In the text it is shown that this is allowed.

The calculations in this Section are too complicated to be easily done by hand. We have had to resort to the use of MAPLE for symbolic manipulation of complicated expressions. We will give substantial details for the first of these calculations, but after that we will omit the proofs. There is a good reason to perform algebraic manipulations rather than the less painful strictly numerical calculations (see the Appendix). A detailed numerical study for many more jump number sequences is desirable but outside the scope of the present work.

We first turn our attention to the existence of the (0011) orbit (see Fig. 6.1). For a k-periodic sequence $(n_0, \ldots, n_{k-1})$, we define $(\sum n) \equiv \sum_{i=0}^{k-1} n_i$.

Theorem 6.1. *Fix e_t and e_n in $(0, 1)^2$. Orbits with jump-number sequence $(0, 0, 1, 1)$ exist if and only if (e_t, e_n) is in the small (white) region indicated in Fig. 6.2.*

Sketch of Proof. To avoid confusion between e_t and e_n in the calculations, we set $x \equiv e_t$ and $y \equiv e_n$ for the remainder of this proof. We follow the method set out in Section 5 with one additional computational nicety. It turns out (see below) that all expressions involved are a quotient of two functions. Each of these functions is the sum of a polynomial in x, y, and roots of such polynomials. To facilitate computations done in MAPLE we carefully separate the numerator and denominator of these expressions.

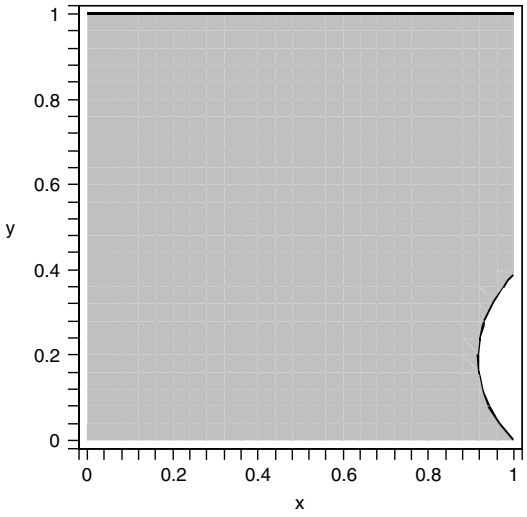

Fig. 6.2. The (0011) orbit exists only where the value of the function $\Delta z_3 - 4\kappa_{(0011)}(u_3+v_3)v_3$ is negative. That happens if and only if the pair $(e_t, e_n) \equiv (x, y)$ is in the white area. (Horizontal axis: $x \in [0, 1]$; vertical axis: $y \in [0, 1]$).

To simplify notation, we set $\{m, n\} \equiv \sqrt{y^m + y^n}$ and simplify up to radicals — that is: $\{2, 4\} = y\{0, 2\}$ and so forth. From the formulas in the introduction of this section one derives the expressions for v_i and $\sqrt{v_i^2 + n_i}$ easily enough. The result is the following. These expressions are given in the tables below; they share the same denominator (the multipliers given in the header of the tables).

Multiply by $(1-y^8)^{-1/2}$		Multiply by $(1-y^8)^{-1/2}$	
v_0:	$y\{0,2\}$	$\sqrt{v_0^2+n_0}$:	$y\{0,2\}$
v_1:	$y^2\{0,2\}$	$\sqrt{v_1^2+n_1}$:	$y^2\{0,2\}$
v_2:	$y^3\{0,2\}$	$\sqrt{v_2^2+n_2}$:	$\{0,6\}$
v_3:	$y\{0,6\}$	$\sqrt{v_3^2+n_3}$:	$\{0,2\}$

So, for example, from these two tables we read off that

$$\sqrt{v_0^2+n_0} = v_0 = \frac{y\sqrt{1+y^2}}{\sqrt{1-y^8}}.$$

From this we obtain:

Multiply by $(1-x^4)^{-1}(1-y^8)^{-1/2}$

$$\begin{aligned}
u_0:&\quad x\Big(\{0,2\}+y\{0,6\}\Big)+x^2\Big(y^3\{0,2\}+\{0,6\}\Big)\\
&\quad +x^3\Big(2y^2\{0,2\}\Big)+x^4\Big(2y\{0,2\}\Big)\\
u_0:&\quad x^2\Big(\{0,2\}+y\{0,6\}\Big)+x^3\Big(y^3\{0,2\}+\{0,6\}\Big)\\
&\quad +x^4\Big(2y^2\{0,2\}\Big)+x\Big(2y\{0,2\}\Big)\\
u_0:&\quad x^3\Big(\{0,2\}+y\{0,6\}\Big)+x^4\Big(y^3\{0,2\}+\{0,6\}\Big)\\
&\quad +x\Big(2y^2\{0,2\}\Big)+x^2\Big(2y\{0,2\}\Big)\\
u_0:&\quad x^4\Big(\{0,2\}+y\{0,6\}\Big)+x\Big(y^3\{0,2\}+\{0,6\}\Big)\\
&\quad +x^2\Big(2y^2\{0,2\}\Big)+x^3\Big(2y\{0,2\}\Big)
\end{aligned}$$

Denoting the right hand sides of this table (that is: without the multiplier given in the header of the table!) by U_i, we now get:

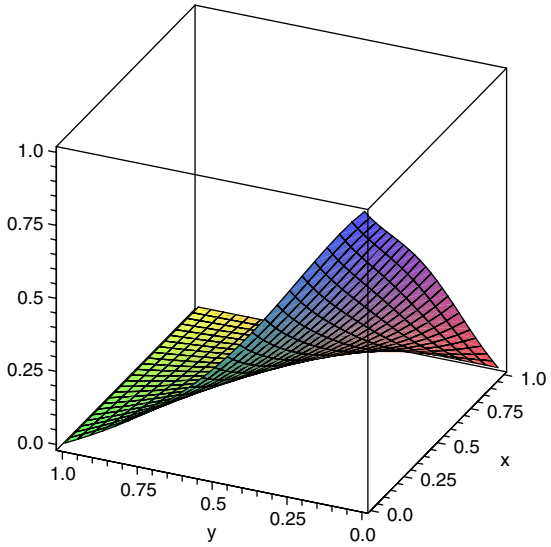

Fig. 6.3. The function $\kappa_{(0011)}$ on the unit square, $(x, y) \in [0, 1]^2$, plotted using MAPLE.

Multiply by $(1-x^4)^{-1}(1-y^8)^{-1}$

$(u_0+v_0)(v_0+\sqrt{v_0^2+n_0})$:	$(U_0+y\{0,2\}(1-x^4))(2y\{0,2\})$
$(u_1+v_1)(v_1+\sqrt{v_1^2+n_1})$:	$(U_1+y^2\{0,2\}(1-x^4))(2y^2\{0,2\})$
$(u_2+v_2)(v_2+\sqrt{v_2^2+n_2})$:	$(U_2+y^3\{0,2\}(1-x^4))(y^3\{0,2\}+\{0,6\})$
$(u_3+v_3)(v_3+\sqrt{v_3^2+n_3})$:	$(U_3+y\{0,6\}(1-x^4))(y\{0,6\}+\{0,2\})$

For the right-hand sides of this last table, write L_i (without the multiplier!), and write $D \equiv (1-x^4)(1-y^8)$. Finally set $Q \equiv \sum L_i$. One then derives that

$$\kappa_{(0011)} = \frac{(\sum n)D}{(\sum n)D+2Q} = \frac{D}{D+Q}.$$

Or:

$$\begin{aligned}
&\frac{(1-x^4)(1-y^8)}{\kappa_{(0011)}(x,y)}\\
&\quad=\Big((y+y^3)\{0,2\}\{0,6\}+1+3y^2+4y^4+3y^6+y^8\Big)\\
&\qquad+\Big((1+4y^2+y^4)\{0,2\}\{0,6\}+3y+7y^3+7y^5+3y^7\Big)x\\
&\qquad+\Big((4y+4y^3)\{0,2\}\{0,6\}+4y^2+8y^4+4y^6\Big)x^2\\
&\qquad+\Big((1+4y^2+y^4)\{0,2\}\{0,6\}+3y+7y^3+7y^5+3y^7\Big)x^3\\
&\qquad+\Big((y+y^3)\{0,2\}\{0,6\}+1+3y^2+4y^4+3y^6+y^8\Big)x^4.
\end{aligned}$$

Or more succinctly as in Fig. 6.3.

At any rate, it is clear that:

$$\begin{aligned}
\Delta z_i &= (1-\kappa_{(0011)})n_{i-1} - 2\kappa_{(0011)}\frac{L_{i-1}}{D}\\
&= \left(1-\frac{(\sum n)D}{(\sum n)D+2Q}\right)n_{i-1} - 2\frac{(\sum n)D}{(\sum n)D+2Q}\frac{L_{i-1}}{D}
\end{aligned}$$

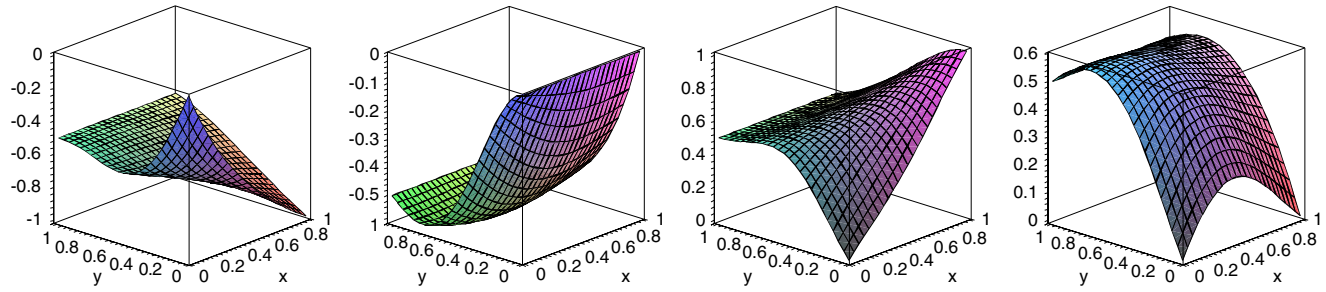

Fig. 6.4. The functions Δz_0, Δz_1, Δz_2, and Δz_3 on the unit square, $(x, y) \in [0, 1]^2$, plotted using MAPLE.

$$= \frac{2Qn_{i-1} - 2(\sum n)L_{i-1}}{(\sum n)D + 2Q}.$$

By inspecting the plots of Δz_i in Fig. 6.4, it becomes clear that Δz_1 and Δz_2 are negative while the other two are positive. (To actually prove this might be an algebraic challenge, but it is not very interesting from a dynamical point of view.) Thus without loss of generality (by local translation invariance) we take

$$z_2 = 0.$$

Now the conditions (recall Lemma (2.6)) to be satisfied for the existence of a (0011) orbit reduce to only two equations, namely replace the jump number by 0 in those equations where it is supposed to be 1:

$$h_2(0) \equiv z_2 - 2\kappa_{(0011)}(u_2 + v_2)(2v_2) < 0 \quad \text{and}$$
$$h_3(0) \equiv z_3 - 2\kappa_{(0011)}(u_3 + v_3)(2v_3) < 0.$$

Note that these two expressions are functions of x and y. Since, as observed, we may take $z_2 = 0$, the first condition is clearly satisfied. In the second equation we substitute $\Delta z_3 = z_3 - z_2$ for z_3. For (x, y) in $(0, 1)^2$, it is satisfied only when x is very close to 1 while y must be relatively small. Illustrations of this can be seen in Fig. 6.2, where the function h is depicted. The function h is too complicated to be conveniently exhibited here, and the actual proof of these inequalities may be challenging but bears no direct relation to the problem at hand. We just mention here that the value of the depicted function at $(x, y) = (1, 1/4)$ equals about -3×10^{-2}. ■

Theorem 6.2. *Fix e_t and e_n in $(0, 1)^2$. Orbits with jump number sequence $(0, 1, 1)$ exist if and only if (e_t, e_n) is in the white region indicated in Fig. 6.5.*

The proof is very similar to the one given before. We only give the function $\kappa_{(011)}(x, y)$ here (recall that we set $e_t = x$ and $e_n = y$ and $\sqrt{1 + y^2}$ is written as $\{0, 2\}$).

$$\begin{aligned}
&\frac{(1 - x^3)(1 - y^6)}{\kappa_{(0011)}(x, y)} \\
&= \Big((y + y^2)\{0, 2\}\{0, 4\} + 1 + 3y^2 + 3y^4 + y^6\Big) \\
&\quad + \Big((1 + 2y + 2y^2 + y^4)\{0, 2\}\{0, 4\} + 3y + 4y^3 + y^4 + 3y^5\Big)x \\
&\quad + \Big((1 + 2y + 2y^2 + y^4)\{0, 2\}\{0, 4\} + 3y + 4y^3 + y^4 + 3y^5\Big)x^2 \\
&\quad + \Big((y + y^2)\{0, 2\}\{0, 4\} + 1 + 3y^2 + 3y^4 + y^6\Big)x^3.
\end{aligned}$$

Notice that Lemma 5.3 implies that orbits with jump number sequences (0022) or (022) exist in a region even smaller than the regions of existence for orbits with jump number sequences (0011) or (011). The system prefers orbits with jump number sequences whose greatest common denominator equals 1. We will look at an example of this phenomenon and analyze the criteria of existence of orbits with jump number sequence $m\{0, 1, 0, 1\cdots\}$. After substitution and some manipulation, we see that (compare with [36]):

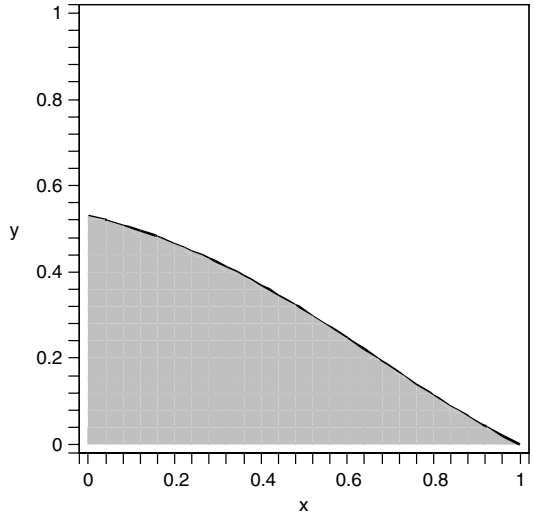

Fig. 6.5. The (011) orbit exists if and only if the pair $(e_t, e_n) \equiv (x, y)$ is in the white region. (Horizontal axis: $x \in [0, 1]$; vertical axis: $y \in [0, 1]$).

$$\kappa_{m(01)} = \kappa_{(01)} \equiv \frac{(1 - e_t^2)(1 - e_n^4)}{(1 + e_t^2)(1 + 6e_n^2 + e_n^4) + 8e_te_n(1 + e_n^2)}.$$

Theorem 6.3. *Fix e_t and e_n in $(0, 1)^2$. Orbits with jump number sequence $(0m)$ for $m \geq 2$ may exist if and only if (e_t, e_n) is in the white regions indicated in Fig. 6.6 (for $m \in \{2, 3, 4, 6\}$ only).*

Remark. The proof entirely follows the outline given in Section 5.

Finally, we compare the values of κ for the various types of periodic orbit so far encountered. The importance of this result lies mostly in the two observations. The first is that, without exception, these data indicate that the rotation number (when defined) appears to be a non-increasing function of κ. The second is that it supports the main Conjecture 2.2. Here are the details.

Theorem 6.4. *Denote an arbitrary periodic jump number sequence by σ. We have the following relations on: κ_∞, $\kappa_{(1)}$, $\kappa_{(m,m+1)}$, $\kappa_{(01)}$, $\kappa_{(0011)}$, $\kappa_{(0^k1)}$, and κ_s:*

1. *For all σ and $\in \mathbb{N}$, $\kappa_{m\sigma} = \kappa_\sigma$.*
2. *The above functions satisfy the obvious compatibility relations (where the corresponding periodic orbits are defined). For example for $m = 0$ and $k = 1$, $\kappa_{(m,m+1)}$ and $\kappa_{(0^k1)}$ are equal and $\kappa_\infty = \kappa_{(1)}$.*
3. *Let σ be one of the non-constant jump numbers considered in this Theorem. We have that $\kappa_\infty < \kappa_\sigma < \kappa_s$.*

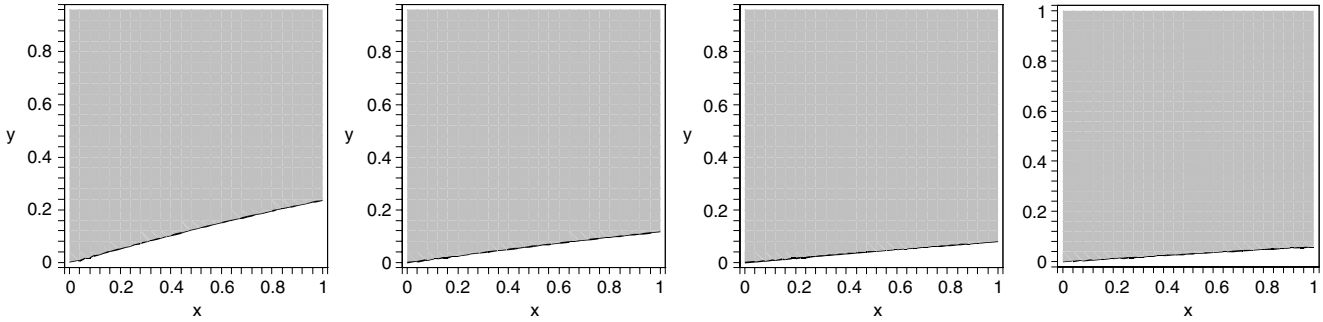

Fig. 6.6. The regions of existence (white) of orbits with jump number sequence (02), (03), (04), and (05), respectively ($x \equiv e_t$ and $y \equiv e_n$). (Horizontal axis: $x \in [0, 1]$; vertical axis: $y \in [0, 1]$).

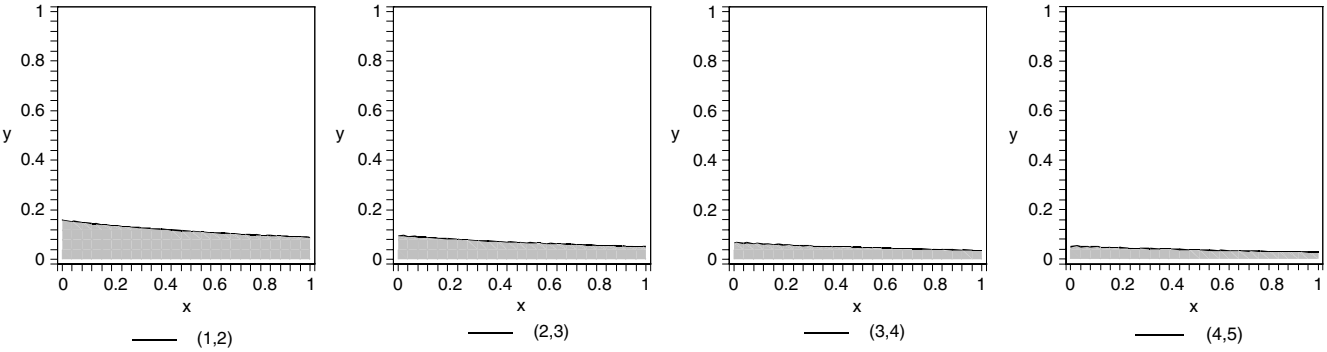

Fig. A.1. The regions of existence (white) of orbits with jump number sequence (1, 2), (2, 3), (3, 4), and (4, 5), respectively ($x \equiv e_t$ and $y \equiv e_n$). (Horizontal axis: $x \in [0, 1]$; vertical axis: $y \in [0, 1]$).

4. *The following compares certain periodic orbits (wherever defined) with one another. The arrows indicate pointwise convergence.*

$$\kappa_\infty \longleftarrow \cdots < \kappa_{(3,4)} < \kappa_{(2,3)} < \kappa_{(1,2)} < \kappa_{(01)} < \kappa_{(001)} < \kappa_{(0001)} < \cdots \longrightarrow \kappa_S.$$

5. *The following compares orbits with jump number sequences* (011) *and* (0011) *(only where defined) with the ones in item 4.*

$$\kappa_{(1,2)} < \kappa_{(011)} < \kappa_{(01)}.$$

$$\kappa_{(01)} < \kappa_{(0011)} < \kappa_{(001)}.$$

Remarks on the Proof. Statement 1 has been mentioned before; it is collected here for reasons of completeness. Statement 2 merely follows from the definitions of the various functions denoted using the letter κ and Theorem 5.1. Statement 4 was proved (though not explicitly stated) in [36]. Statement 3 is implied by 4 and 5. Statement 5 is essentially too hard to do conveniently by hand, and we took recourse to MAPLE. ■

Acknowledgements

We want to thank Juan Campos for many useful comments such as, among other things, one that resulted in the erratum contained in this paper. In addition, JJPV gratefully acknowledges a fellowship granted by the Spanish Government through its Ministry of Science and Education enabling him to dedicate an academic year to research while based in Granada, Spain. JJPV also thanks Lluis Alsedà, Eddie G. D. Cohen, and Giovani Vasconcelos for useful if not illuminating conversations.

Partially supported by a MCYT/FEDER grant number MTM2008-02502, and a grant number FQM2216 from Junta de Andalucía.

Appendix

One of our aims in Section 6 is precisely to exhibit some of the formulae so that algebraic regularities in them can be spotted, which could eventually lead to the analytical reasons for this curious preference of orbits with order preserving jump number sequences. They may point to important new directions in the analysis of these systems.

Order preserving sequences describe the symbolic dynamics of invertible circle maps of degree 1 (whose orbits have the property that they are order preserving ie: they cannot "cross"). Essentially all order preserving sequences consisting of only 0's and 1's can be obtained by fixing $\rho \in [0, 1]$ and $d \in [0, 1)$. Now the nth symbol σ_n of the binary sequence σ equals 1 if $[(n-1)\rho + d)$ contains an integer and equal 0 if that is not the case. All these sequences have the property that $\lim_{n\to\infty} \sum_1^n \sigma_i = \rho$, the so-called rotation number. The set of order preserving sequences with rotation number ρ will be denoted by Σ_ρ. Similar constructions work for sequences consisting of digits k and $k+1$, any $k \in \mathbb{N}$.

Sequences in Σ_ρ have a certain 'optimality' property. Namely, for all $\sigma \in \Sigma_\rho$ and all $q \in \mathbb{N}$, every subsequence of length q in σ has either p or $p+1$ 1's in it, where p is such that $\rho \in (\frac{p}{q}, \frac{p+1}{q})$. (If $\rho = \frac{p}{q}$ then every q subsequent have exactly p 1's in them.) These statements can be made precise and proved (see [43,44]).

The point is that fluctuations in the running mean of 1's in these sequences is minimal. The relation between the speed of a particle and its jump number sequence (given in Eqs. (5.1) and (5.2) for periodic sequences) is not simple. But one can nonetheless make the inference that "larger" jump numbers lead to larger speeds. Consequently one expects the speed along an orbit to vary less if its jump number sequence is order preserving than for one that violates order preserving.

The preference for orbits with order preserving jump number sequences leads (heuristically) to the conclusion that within a a group of objects all falling together down a slope (an avalanche), the number of internal collisions (and their relative energies) might be much less than in that of a group of objects that perform a random motion with a drift. This has far-reaching consequences

in the physical description of the conglomerate of these objects. In particular, internal energy dissipation (that is: the ones resulting from object-object collision) will be small, so that the motion of the conglomerate will have aspects of that of a fluid or a gas (which is indeed attested in some of the cited literature).

A.1. Erratum to Proposition 7 of [36]

Proposition 7 of [36] contains a mistake. That Proposition should run as follows:

Proposition A.1. *Orbits with jump number sequence* $(0, 1)$ *exist for all* $(e_t, e_n) \in (0, 1)^2$. *For jump sequences* $(m, m+1)$ *with* $0 < m < 5$, *the corresponding orbits exists except in a region where* e_n *is small (see Fig.* A.1*).*

Remark. Presumably for larger m the regions of non-existence get smaller. We have tested this (affirmatively) for $m = 10$ and 20 (evidence not shown).

References

[1] R.M. Nedderman, Statics and Kinematics of Granular Materials, Cambridge University Press, 1992.
[2] G.L. Vasconcelos, F.V. Cunha Jr., J.J.P. Veerman, Chaotic behavior in a model for grain dynamics, Physica A 295 (2001) 261–267.
[3] J. Campos, M.J. Romero-Vallés, P.J. Torres, J.J.P. Veerman, Dynamics of a jumping particle on a staircase profile, Chaos Solitons Fractals 32 (2) (2007) 415–426.
[4] J.J.P. Veerman, A solvable model for gravity driven granular dynamics, Dyn. Syst. 20 (2) (2005) 237–254, doi:10.1080/14689360500091191.
[5] G.L. Vasconcelos, J.J.P. Veerman, Geometrical model for a particle on a rough inclined surface, Phys. Rev. E 59 (1999) 5641–5646.
[6] H.M. Jaeger, C.-h. Liu, S.R. Nagel, Relaxation at the angle of repose, Phys. Rev. Lett. 62 (1) (1989) 40–43.
[7] V. Frette, K. Christensen, A. Malthe-Sørenssen, J. Feder, T. Jøssang, P. Meakin, Avalanche dynamics in a pile of rice, Nature 379 (1996) 49–52.
[8] H.J. Hermann, J.-P. Hovi, S. Luding (Eds.), Physics of Dry Granular Media, in: NATO ASI Series E: Applied Sciences, vol. 350, Kluwer, 1998.
[9] H.M. Jaeger, S.R. Nagel, R.P. Behringer, The physics of granular materials, Physics Today (April) (1996) 32–38.
[10] H.M. Jaeger, S.R. Nagel, R.P. Behringer, Granular solids, liquids and gases, Rev. Modern Phys. 68 (4) (1996) 1259–1273.
[11] P.A. Lemieux, D.J. Durian, From avalanches to fluid flow: A continuous picture of grain dynamics down a heap, Phys. Rev. Lett. 85 (20) (2000) 4273–4276.
[12] J. Lee, Avalanches in $1 + 1$ dynamical piles: A molecular dynamics study, J. Phys. I 3 (1993) 2017–2027.
[13] C. Henrique, M.A. Aguirre, A. Calvo, I. Ippolito, S. Dippel, G.G. Batrouni, D. Bideau, Energy dissipation and trapping of particles moving on a rough surface, Phys. Rev. E 57 (1998) 4743.
[14] L. Samson, I. Ippoliti, D. Bideau, G.G. Batrouni, Motions of grains down a bumpy surface, Chaos 9 (3) (1999) 639–648.
[15] G. Ristow, F.X. Riguidel, D. Bideau, different characteristics of the motion of a single particle on a bumpy inclined line, J. Phys. I 4 (1994) 1161.
[16] M.P. Almeida, J.S. Andrade Jr., H.J. Herrmann, Aeolian transport layer, Phys. Rev. Lett. (1) (2006) 018001.
[17] J. Hermans, A symmetric sphere rolling on a surface, Nonlinearity 8 (4) (1995) 493–515.
[18] S.J. Hogan, On the dynamics of rigid-block motion under harmonic forcing, Proc. Roy. Soc London Ser. 425 (1869) (1989) 441–476.
[19] R.I. Leine, D.H. Van Campen, B.L. Van de Vrande, Bifurcations in nonlinear discontinuous systems, Nonlinear Dynam. 23 (2000) 105–164.
[20] J.M. Alonso, R. Ortega, Roots of unity and unbounded motions of an asymmetric oscillator, J. Differential Equations 143 (1998) 201–220.
[21] R. Ortega, Boundedness in a piecewise linear oscillator and a variant of the small twist theorem, Proc. London Math. Soc. 79 (1999) 381–413.
[22] A.C. Lazer, J.P. McKenna, Large amplitude periodic oscillations in suspension bridges: Some new connections with nonlinear analysis, SIAM Rev. 32 (1990) 537–578.
[23] A.F. Filippov, Differential Equations with Discontonuous Righthand Sides, Kluwer Ac. Pub., London, 1988.
[24] K. Deimling, Resonance and coulomb friction, Differ. Integral Equ. 7 (1994) 759–765.
[25] K. Deimling, P. Szilagyi, Periodic solutions of dry friction problems, Z. Angew. Math. Phys. 45 (1994) 53–60.
[26] M. Kunze, T. Küpper, Qualitative bifurcation analysis of a non-smooth Friction–Oscillator model, Z. Angew. Math. Phys. 48 (1997) 87–101.
[27] G. Olivar, E. Fossas, C. Batlle, Bifurcations and chaos in converters. discontinuous vectorfields and singular poincaré maps, Nonlinearity 13 (4) (2000) 1095–1121.
[28] E. Fermi, On the origin of cosmic radiation, Phys. Rev. 75 (1949) 1169–1174.
[29] P.C. Tung, S.W. Shaw, The dynamics of an impact print hammer, ASME J. Vib. Stress Reliab. Des. 110 (1988) 193–199.
[30] E. Gutkin, Billiard dynamics: A survey with the emphasis on open problems, Regul. Chaotic Dyn. 8 (1) (2003) 1–13.
[31] M.L. Ferguson, B.N. Miller, M.A. Thompson, Dynamics of a gravitational billiard with a hyperbolic lower boundary, Chaos 9 (4) (1999) 841–848.
[32] S. Feldt, J.S. Olafsen, Inelastic gravitational billiards, Phys. Rev. Lett. 94 (2005) 224102.
[33] K. Popp, Non-smooth mechanical systems, J. Appl. Math. Mech. 64 (2000) 765–772.
[34] V.I. Babitsky, Theory of Vibro-impact Systems and Applications, Springer, 1998.
[35] M. Kunze, Non-smooth Dynamical Systems, in: Lecture Notes in Mathematics, vol. 1744, Springer-Verlag, Berlin, 2000.
[36] J.J.P. Veerman, F.V. Cunha Jr., G.L. Vasconcelos, Dynamics of a granular particle on a rough surface with a staircase profile, Physica D 168–169 (2002) 220–234.
[37] V. Berger, T. Schwager, T. Pöschel, Coefficient of tangent restitution for the linear dashpot model, Phys. Rev. E77 (2008) 011304.
[38] R. Cross, The coefficient of restitution for happy balls, unhappy balls, and tennis balls, Amer. J. Phys. 68 (11) (2000) 1025–1031.
[39] J. Milnor, On the concept of attractor, Comm. Math. Phys. 99 (1985) 177–195.
[40] J. Milnor, On the concept of attractor: Correction and remarks, Comm. Math. Phys. 102 (3) (1985) 517–519.
[41] A. Valance, D. Bideau, Dynamics of a ball on a rough inclined line, Phys. Rev. E 57 (1998) 1886.
[42] A. Cima, A. Gasull, F. Mañosas, The discrete Markus–Yamabe problem, Nonlinear Anal. 35 (3) (1999) 343–354.
[43] J.J.P. Veerman, Symbolic dynamics and rotation numbers, Physica A 13 (1986) 543–576.
[44] J.J.P. Veerman, Symbolic dynamics of order-preserving orbits, Physica D 29 (1987) 191–201.
[45] J.J.P. Veerman, F.M. Tangerman, Renormalization of Aubry–Mather cantor sets, J. Statist. Phys. 56 (1–2) (1989) 83–98.